Threonine[6]-Bradykinin: Structural Characterization in the Presence of Micelles by Nuclear Magnetic Resonance and Distance Geometry†

Maria Pellegrini,‡,§ Stefano Mammi,§ Evaristo Peggion,§ and Dale F. Mierke*,‡,||

Gustaf H. Carlson School of Chemistry, Clark University, 950 Main Street, Worcester, Massachusetts 01610, Department of Organic Chemistry, University of Padova, Biopolymer Research Center, Via Marzolo 1, Padova, Italy I-35131, and Department of Pharmacology and Molecular Toxicology, University of Massachusetts, Medical Center, 55 Lake Avenue North, Worcester, Massachusetts 01655

Received July 25, 1996⊗

The conformation of the natural peptide [Thr[6]]-bradykinin, Arg[1]-Pro[2]-Pro[3]-Gly[4]-Phe[5]-Thr[6]-Pro[7]-Phe[8]-Arg[9], is investigated by NMR spectroscopy and computer simulations in an aqueous solution of sodium dodecyl sulfate micelles. The structural analysis of the peptide is of particular interest since it displays a different biological profile from bradykinin despite the high sequence homology (only one conservative substitution: Ser[6]/Thr[6]) and the fact that both peptides bind and activate common receptors. The SDS micelles provide a model system for the membrane−interface environment the peptide experiences when interacting with the membrane-embedded receptor and allow for the conformational examination of the peptide using high-resolution NMR techniques. The NMR spectra show that the micellar system induces a secondary structure in the otherwise inherently flexible peptide (as observed in benign aqueous solution). The distance geometry calculations indicate a β-turn of type I about residues 7−8 as the preferred conformation. The results of ensemble calculations reveal conformational changes occurring rapidly on the NMR time scale and allow for the identification of three different families of conformations that average to reproduce the NMR observables. The three families differ in the type of conformation adopted at the C-terminus: type I β-turn, type II β-turn and a third conformation, intermediate between the two β-turns. The structural results support the hypothesis of the determining role of the C-terminal conformation for biological activity and can provide an explanation of the different activities observed for bradykinin and [Thr[6]]-bradykinin.

Introduction

Bradykinin (BK; Arg[1]-Pro[2]-Pro[3]-Gly[4]-Phe[5]-Ser[6]-Pro[7]-Phe[8]-Arg[9]) is a linear nonapeptide hormone produced by enzymatic cleavage of its high molecular weight precursor, kininogen, at the occurrence of tissue injury or trauma.[1] The role of the peptide in the regulation of major physiological systems as well as in a wide variety of pathological responses has been demonstrated (for a recent review, see ref 2). It is one of the most potent vasodilators and increases vascular permeability.[3,4] BK also elicits contraction of smooth muscles of the respiratory and gastrointestinal tract and the uterus.[5] BK is active in the central nervous system, where it initiates pain stimuli[6] and is responsible for the cardinal symptoms of inflammation.[7] Recently BK has been associated with the symptoms of the common cold.[8,9]

The conformational analysis of BK, BK fragments, and analogs is the object of considerable interest with the aim of gaining insight into a possible bioactive conformation and development of a structure−activity relationship. The general conclusion of conformational studies in aqueous solution is that BK exists in many conformational states.[10] However, in alternative solvent systems the inherently flexible nonapeptide preferred folded conformations. In the absence of X-ray crystallography or NMR data on the structure of the peptide when complexed to its receptor, one must rely on such studies, possibly in a solvent that mimics the biological environment the peptide experiences when bound to the receptor, to establish possible bioactive secondary structure(s).

The receptor for BK (at least two classes have been identified)[2] belongs to the family of G-protein-coupled receptors, characterized by seven transmembrane hydrophobic helical segments. A membrane-bound pathway for the interaction between the peptide hormones and their receptors has been hypothesized;[11,12] the mechanism implies the accumulation and orientation of the peptide on the membrane, thus increasing the local concentration and at the same time reducing the degrees of rotational and translational freedom (i.e., reduction from 3D diffusion to a lateral, 2D diffusion).[13−15] This could also facilitate the transition from the random coil structure, usually adopted by the peptides in the extracellular solution, to the bioactive conformation.[16−18]

The NMR study of peptides incorporated into membranes is extremely difficult, owing to the drastic line broadening, the high concentration of the lipid compared to the embedded peptide, and the overlap of signals. Therefore micellar systems have been often used to mimic a membrane-like environment which may induce biologically relevant conformations in oligopeptides[19,20] and is suitable for NMR studies.[21−26]

† Abbreviations: BK, bradykinin; [Thr[6]]-BK, threonine[6]-bradykinin; NMR, nuclear magnetic resonance; NOEs, nuclear Overhauser enhancements; SDS, sodium dodecyl sulfate; DG, distance geometry; DADD, distance- and angle-driven dynamics.

* To whom correspondence should be addressed at Clark University. Tel: (508) 793-7220. Fax: (508) 793-8861. E-mail: dmierke@clarku.edu.
‡ Clark University.
§ University of Padova.
|| University of Massachusetts.

⊗ Abstract published in *Advance ACS Abstracts,* December 15, 1996.

S0022-2623(96)00539-0 CCC: $14.00

Table 1. Proton Chemical Shifts (Referenced to internal tetramethylsilane, $T = 308$ K), HN−Hα Coupling Constants, and HN Temperature Coefficients of [Thr6]-BK in H_2O in the Presence of SDS Micelles

residue	HN	H^α	H^β	H^γ	others	J (Hz)	$\Delta\delta/\Delta T$ (−ppb/K)
Arg1		4.42	1.88, 2.04	1.88, 2.04	δ 3.29; εHN 7.32		
Pro2		4.94	2.04, 2.56		δ 3.52, 3.90		
Pro3		4.48	2.03, 2.35	2.14	δ 3.81, 3.93		
Gly4	8.21	3.99				Σ = 11.2	7.2
Phe5	7.83		3.10, 3.17		Ar 7.29	7.3	4.3
Thr6	7.94	4.64	4.18	1.20	OH −	7.9	6.5
Pro7		4.32	1.68, 2.20	1.77	δ 3.35, 3.57		
Phe8	7.91		3.18, 3.31		Ar 7.42	7.9	7.9
Arg9	7.85	4.47	1.74, 2.04	1.74, 2.04	δ 3.30; εHN 7.18	7.5	3.2

The conformational study of BK in aqueous solution in the presence of sodium dodecyl sulfate (SDS) micelles has been reported by Lee and co-workers.[27] The peptide adopts a folded conformation in the C-terminal region, between Ser6 and Arg9, that from distance geometry and molecular dynamics calculations has been identified as a β-turn-like structure. This result, combined with other conformational studies in solution on BK itself and on peptidic agonists and antagonists, led to the hypothesis that a β-turn in the four C-terminal amino acids is a prerequisite for activity and that the type of β-turn adopted is related to the difference between agonist and antagonist, together with the required orientation of the side chains.[28−33]

[Thr6]-Bradykinin, [Thr6]-BK, was discovered in the venom of a solitary wasp[34] in 1983. The venom leads to an immediate and permanent block of transmission at the presynaptic level.[35] In the insect central nervous system (CNS) [Thr6]-BK proved to be 10 times more potent than BK, despite the single, conservative substitution in the sequence.[36,37] The presence of [Thr6]-BK and other BK-like peptides in wasp and ant venom and frog skin also suggests a toxic effect in vertebrates, although the mode of action on mammalian CNS is still obscure.[36]

The peptide has been tested for the capability of stimulating smooth muscle contraction, and the results have been compared with those for BK. Its potency in causing the contraction of the guinea pig rectum is 10 times higher than for BK, tested in the same experiment.[38]

Here we present the results on the natural peptide [Thr6]-BK, which was investigated in water and SDS micelles by NMR spectroscopy. To our knowledge this is the first conformational study of [Thr6]-BK (a parallel study of [Thr6]-BK in dimethyl sulfoxide has been recently completed; see: Pellegrini et al., manuscript in preparation). Our goal is the development of high-quality three-dimensional structures of the peptide in the micellar solution to allow for greater insight, on a structural basis, into the differences in activity observed between BK and [Thr6]-BK.

In addition, since [Thr6]-BK is a small linear and therefore flexible peptide, we consider the examination of the possibility of conformational changes occurring fast on the NMR time scale of extreme importance. When this is the case, the NMR observables, and restraints developed from them, will be consistent with an average structure that may not exist in solution or is not physically possible. The idea of "the structure" is no more suitable, and an ensemble of conformations must be taken into account to explain the experimental data. When dealing with a highly flexible system it is therefore imperative to apply the NMR restraints as averages over multiple copies of the molecules. Using the ensemble approach, different families of conformations are obtained for the C-terminal portion of the peptide [Thr6]-BK.

Experimental Procedures

Nuclear Magnetic Resonance. The NMR experiments have been carried out on a 4.1 mM sample (based on weight) in aqueous solution (90% H_2O−10% D_2O; Cambridge Isotopes) containing 200 mM SDS-d_{25} (98.6%; MSD Isotopes). The molar ratio of peptide/detergent was used to obtain an approximate occurrence of 1 peptide molecule/micelle.[39] The final pH of the solution was 4.5 (not corrected for isotope effect). Proton spectra were recorded on a Varian Unity 500 MHz spectrometer and processed using Varian VNMR software or *Felix* (Biosym Technologies Inc., San Diego). Chemical shifts were calibrated with respect to internal tetramethylsilane.

For assignment of the spin systems, DQF-COSY,[40] TOCSY,[41,42] and NOESY[43,44] spectra were recorded in the phase-sensitive mode using the method from States.[45] A ROESY[46] spectrum with a mixing time of 200 ms was recorded in order to identify exchange phenomena for HN−HN and H^α−H^α cross-peaks of the NOESY spectrum; a spin−lock field of 2500 Hz was realized by a series of short pulses as described by Kessler[47] sandwiched between two 90° pulses to compensate for offset effects (compensated ROESY). NOESY spectra were collected at 308 K with mixing times varying from 100 to 200 ms. Suppression of the solvent signal was achieved by continuous wave presaturation at low power during the relaxation delay (1.2−2 s) and for NOESY experiments also during the mixing time. The typical spectral width was 5000 Hz in both dimensions; with 2048 data points in t_2 and 512 data points in t_1, and 32−128 scans at each increment. Forward linear prediction to 1024 points and zero-filling to 2048 were applied to the incremented dimension; Gaussian apodization was used in both t_2 and t_1. For the temperature coefficients measurement 1D spectra were recorded at $T = 308$ and 313 K. For overlapping resonances it was necessary to acquire TOCSY spectra at 298, 303, and 318 K (4096 points in t_2, 256 in t_1, and 4 scans/increment). The complete proton assignment is given in Table 1.

For determination of homonuclear coupling constants, the PE COSY[48] pulse sequence was employed. The spectrum was acquired at 308 K with 4096 data points in t_2 and 640 incremental data points. The t_2 dimension was expanded with zero-filling to 8196 points.

Cross-peak volumes from the 200 ms NOESY spectrum were obtained using *Felix*, within the *Insight II* suite of programs (Biosym Technologies Inc., San Diego). The volumes were converted to distances using the isolated two-spin approximation and utilizing the cross-peaks between the two β-methylene protons of each of the prolines as a reference (1.78 Å). No evidence of spin diffusion was observed up to a mixing time of 200 ms. The distances were adjusted by ±10% to produce the upper and lower distance restraints (Table 2). Pseudoatoms were used for aromatic protons, methyl groups, and methylene protons that could not be stereospecifically assigned, with the appropriate correction of the upper distance restraint following standard procedures.[49]

Distance Geometry. The distance geometry (DG) calculations were carried out with a home-written program utilizing

Table 2. Interproton Distances (Upper limits, Å) Utilized in the Distance Geometry Calculations of [Thr^6]-BK in the Presence of SDS Micelles

atom 1		atom 2		distance	
Arg^1	ϵHN	Arg^1	γCH$_2$	3.90	
	H$^\alpha$	Pro^2	δCH$_2$	3.66	
Pro^2	H$^\alpha$	Pro^3	δCH$_2$	3.53	
Pro^3	H$^\beta$ProR	Pro^3	δCH$_2$	3.97	
	H$^\beta$ProR	Pro^3	H$^\alpha$	3.57	
	H$^\beta$ProS	Pro^3	δCH$_2$	3.81	
	H$^\alpha$	Gly^4	HN	2.75	
	H$^\beta$ProR	Gly^4	HN	3.65	
	H$^\beta$ProS	Gly^4	HN	3.40	
	γCH$_2$	Gly^4	HN	3.48	
Gly^4	HN	Gly^4	αCH$_2$	2.36	
	αCH$_2$	Phe^5	HN	2.46	
	HN	Phe^5	HN	2.94	
Phe^5	HN	Phe^5	βCH$_2$	3.00	
	H^{ar}	Phe^5	βCH$_2$	5.71	
	HN	Phe^5	H^{ar}	5.76	
	HN	Thr^6	γCH$_3$	4.64	
	βCH$_2$	Thr^6	HN	4.30	
	H^{ar}	Thr^6	HN	5.76	
	HN	Thr^6	HN	3.05	
Thr^6	HN	Thr^6	γCH$_3$	4.21	
	H$^\beta$	Thr^6	γCH$_3$	3.33	
	HN	Pro^7	δCH$_2$	5.16	
	H$^\beta$	Pro^7	δCH$_2$	4.00	
	H$^\beta$	Phe^8	HN	4.50	(*i*, *i*, + 2)
	γCH$_3$	Phe^8	HN	5.11	(*i*, *i*, + 2)
	H$^\beta$	Arg^9	HN	4.50	(*i*, *i*, + 3)
Pro^7	H$^\beta$ProR	Pro^7	H$^\alpha$	2.34	
	H$^\beta$ProS	Pro^7	H$^\alpha$	2.65	
	δCH$_2$	Pro^7	H$^\beta$ProR	4.15	
	H$^\alpha$	Phe^8	HN	2.69	
	H$^\beta$ProS	Phe^8	HN	3.08	
	γCH$_2$	Phe^8	HN	3.75	
	δCH$_2$	Phe^8	HN	4.43	
	H$^\alpha$	Arg^9	HN	3.31	(*i*, *i*, + 2)
Phe^8	HN	Phe^8	βCH$_2$	3.28	
	H^{ar}	Phe^8	βCH$_2$	5.62	
	HN	Phe^8	H^{ar}	5.48	
	βCH$_2$	Arg^9	HN	4.00	
	H^{ar}	Arg^9	HN	5.90	
	HN	Arg^9	HN	3.00	
Arg^9	HN	Arg^9	H$^\alpha$	2.85	
	HN	Arg^9	βCH$_2$	3.10	
	HN	Arg^9	γCH$_2$	3.30	
	H$^\alpha$	Arg^9	βCH$_2$	4.00	
	ϵHN	Arg^9	δCH$_2$	3.72	
	ϵHN	Arg^9	γCH$_2$	4.01	
	ϵNH	Arg^9	βCH$_2$	3.10	

the random metrization algorithm of Havel.[50] Experimentally determined distances which were more restrictive than the geometric distance bounds (holonomic restraints) were added to create a distance matrix.[51] The structures were first embedded in four dimensions and then partially minimized using conjugate gradients followed by distance- and angle-driven dynamics (DADD).[52−54] The DADD simulation was carried out at 1000 K for 50 ps, and then there was a gradual reduction in temperature over the next 30 ps. The DADD procedure utilizes the holonomic and experimental distance restraints plus a chiral penalty function for the generation of the violation "energy" and forces. The resulting structures were then reduced to three dimensions using metrization, and the optimization and DADD procedure were repeated.

The following ensemble calculations are identical with those used for the DADD method, except that the penalty expression for the experimental restraints (NOEs and coupling constants)[55] and the forces calculated from these restraints are generated from an ensemble average. The metrization and refinement of 94 structures required approximately 15 h of CPU using a single processor on a SGI Indigo2 (R4400) workstation, the ensemble calculations about 1 week time, for 470 structures. Energy minimizations and interactive modeling were performed using *Discover* (Consistent Valence Force Field, CVFF91) and *Insight II* (Biosym Technologies Inc., San Diego). Analyses of the structures in terms of hydrogen bond identification, root mean square deviation (rmsd) values, and dihedral angle distribution were performed using home-written programs.

Results

The ^{1}H-NMR spectra revealed the presence of more than one isomer in solution, in slow equilibrium on the NMR time scale. Only the most abundant isomer exhibits complete spin systems for all the residues and therefore was considered in the following study. The relative intensities of resolved peaks in a 1D spectrum indicate that this isomer is present in a ratio of 8:1 to the second most populated of the species. The different isomers originate from *cis/trans* isomerization at the three X−Pro bonds, and exchange cross-peaks were identified in a ROESY spectrum.

In the major isomer all the prolines are in a *trans* configuration, as determined from diagnostic $H^\alpha_i/H^{\delta 1}_{i+1}$ and $H^\alpha_i/H^{\delta 2}_{i+1}$ cross-peaks between the proline residues and the preceding amino acids in a NOESY spectrum. Stereospecific assignments for three prochiral centers (position β of Pro 2, 3, and 7) obtained from the analysis of NOESY and PE COSY spectra were used in the calculations.

A total of 48 informative NOEs have been observed (see Table 2 for the upper distance limits utilized in the calculations). Of these, most are sequential or intra-residue. In the amide region three HN_i/HN_{i+1} connectivities have been assigned to Gly^4/Phe^5, Phe^5/Thr^6, and Phe^8/Arg^9. In the region of correlation between amide and aliphatic protons, there is evidence for a folded conformation at the C-terminus of the peptide: A strong cross-peak is present between Pro$^7{}_{H^\alpha}$ and Arg$^9{}_{HN}$. These $\alpha N(i,i+2)$ NOEs are normally interpreted as arising from β-turn structures.[56−59] The presence of the turn, centered about Pro^7-Phe^8, is further supported by the short Phe$^8{}_{HN}$/Arg$^9{}_{HN}$ distance and by three NOEs from the side chain of Thr^6 to Phe$^8{}_{HN}$ and Arg$^9{}_{HN}$. In Figure 1 an expanded portion of the amide to aliphatic region of a NOESY spectrum is reported, illustrating the relevant NOEs.

The DG calculations produced 94 low-energy structures. The analysis of the backbone dihedral angles ϕ and ψ indicates that the N-terminal part of the molecule does not have a distinct preference for a ordered conformation, as can be easily seen from a plot of the order parameters of these angles (Figure 2). On the contrary the ϕ and ψ values for Pro^7 and Phe^8, represented in the form of Ramachandran maps in Figure 3, point to a type I β-turn extending from Thr^6 to Arg^9, with slight deviation from the standard values for Phe$^8{}_\phi$ ($\phi_{i+1} = -69 \pm 9°$, $\psi_{i+1} = -46 \pm 7°$; $\phi_{i+2} = -58 \pm 33°$, $\psi_{i+2} = 3 \pm 24°$, averaged over the 94 structures).

The structures satisfy the requirements for a hydrogen bond between the carbonyl oxygen of Thr^6 and the HN of Arg^9. This is in agreement with the temperature coefficient measured for the amide proton of Arg^9, which displays the lowest values of the HN present in the peptide. Figure 4 shows the 94 DG structures superimposed using the heavy backbone atoms in the β-turn region (Thr^6−Arg^9). The average pairwise rmsd for the heavy backbone atoms in this region is 0.76 Å.

The analysis of the violations to upper and lower distance restraints reveals only two significant deviations from the imposed values (the violations are

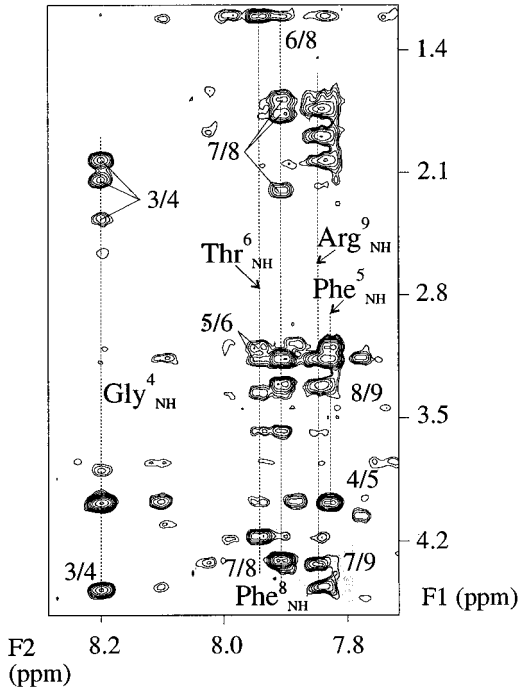

Figure 1. Expanded portion of a NOESY spectrum of [Thr⁶]-BK in water solution with SDS micelles (mixing time = 200 ms, T = 308 K). The region containing some of the relevant NOEs indicating a C-terminal β-turn is shaded.

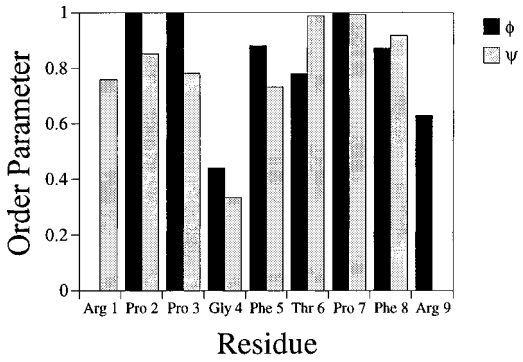

Figure 2. Order parameter values for the ϕ and ψ dihedral angles as obtained from the distance geometry calculations of [Thr⁶]-BK in H_2O/SDS.

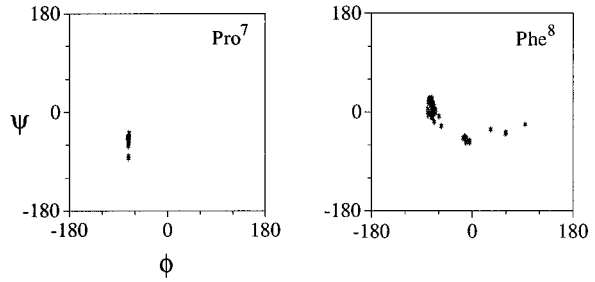

Figure 3. Ramachandran maps for the angles ϕ and ψ for residues 7 and 8 of [Thr⁶]-BK, as obtained from the standard DG calculations.

calculated as an average over the ensemble of structures). Both of them are located in the turn region: $Pro^7{}_{H^\alpha}/Phe^8{}_{HN}$ and $Pro^7{}_{H^\beta}/Phe^8{}_{HN}$, violating the upper distances by 0.35 and 0.28 Å, respectively. The DG structures seem therefore to adequately fulfill the experimental restraints, with the exception of some problems associated with the orientation of the Phe⁸ amide proton: A flip around the ψ dihedral angle of Pro⁷ and ϕ of Phe⁸ would project the amide proton in the opposite direction, generating a type II β-turn that typically displays a shorter distance between the HN of residue $i + 2$ (Phe⁸) and the H^α of residue $i + 1$ (Pro⁷). Nonetheless, the requirement that each structure satisfy all the NOEs produces a homogeneous ensemble with a type I β-turn about residues 7−8 as a favored conformation.

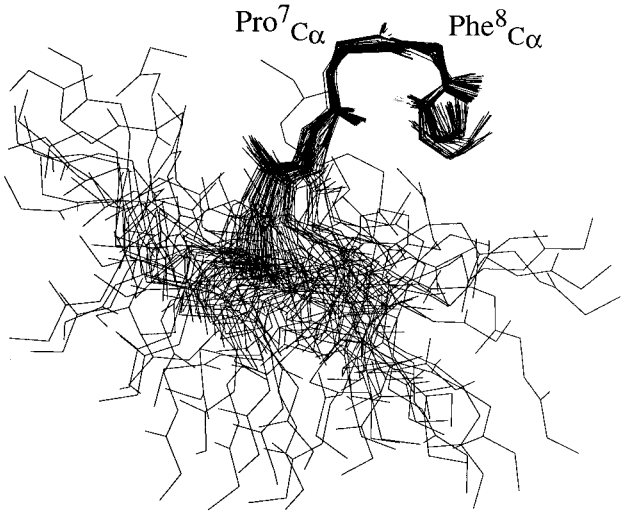

Figure 4. Superposition of the 94 structures of [Thr⁶]-BK obtained from distance geometry calculations. The heavy backbone atoms are superimposed in the region of the C-terminal β-turn, from Ser⁶ to Arg⁹. All backbone atoms (black) and $Phe^8{}_{HN}$ and $Arg^9{}_{HN}$ (gray) are shown.

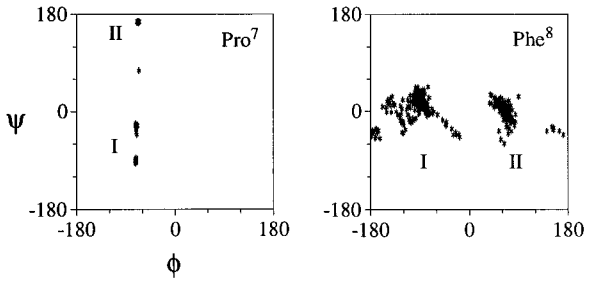

Figure 5. Ramachandran maps for the ϕ and ψ dihedral angles for residues 7 and 8 of [Thr⁶]-BK, as obtained from ensemble calculations.

To examine the possibility that the NMR observables (NOEs and coupling constants) are generated by different conformations in fast equilibrium on the NMR time scale and that this is the cause of the discrepancy between the calculated structures and the experimental distances, ensemble calculations were carried out. The 94 DG structures copied five times constituted the starting ensemble. This is indeed a distorted starting ensemble (i.e., the structures are clustered in the region of the conformational space allowed by the experimental restraints in the classical "one-structure" DG calculations). A nonbiased starting ensemble could be generated by a DG calculation using no restraints; however, this proved not to be necessary because the DADD protocol employed in the ensemble calculations allows the structures to overcome the local energy barriers and sample the conformational space: Simulations run without any NOEs and coupling constants restraints display complete sampling of the ϕ,ψ space.

In the ensemble calculations only the average of the members of the ensemble (470 structures) is required to fulfill the experimental restraints, allowing therefore

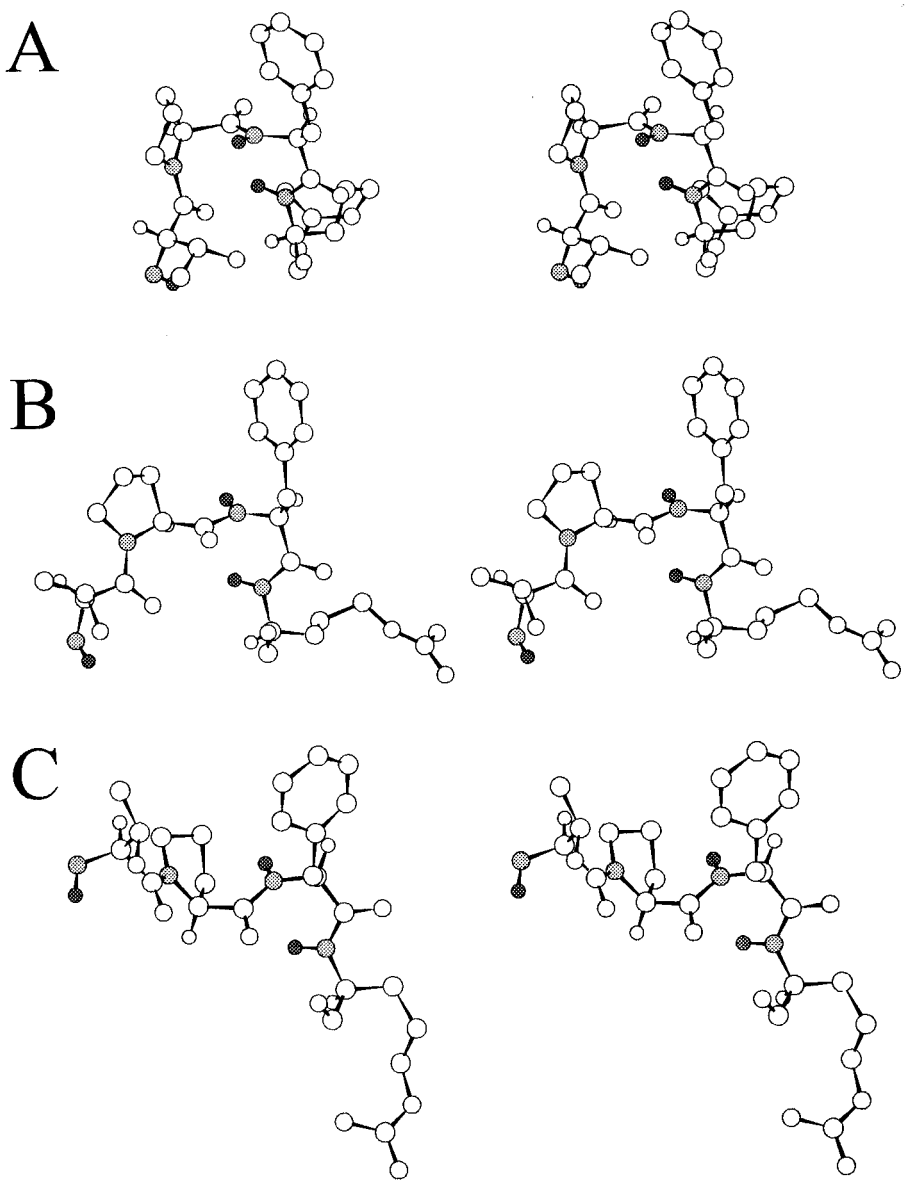

Figure 6. C-terminal turn region of representative structures of the three families of conformations obtained from ensemble calculations: (A) the βI-turn structure, (B) the βII-turn-like structure, and (C) the intermediate, extended structure.

for fast conformational averaging to occur in solution. No violations to upper or lower distance restraints greater than 0.2 Å were observed in the resulting ensemble, and in particular the restraint on the distance $Pro^{7}{}_{H^{\alpha}}/Arg^{9}{}_{HN}$ is fulfilled. The results in the form of ϕ,ψ maps for Pro^{7} and Phe^{8} are shown in Figure 5. Two families of structures can be easily identified from these maps. The first family (labeled as I in the figure) is the one observed from the classic DG calculations corresponding to the type I β-turn. A second group of structures (indicated as II in the figure) clusters around dihedral angle values of a distorted type II β-turn (the angle for $Pro^{7}{}_{\psi}$ deviates from standard values). A third family, which can not be identified from the Ramachandran maps, is intermediate between the other two families (Pro^{7} and Phe^{8} have ϕ,ψ values which belong to families I and II, respectively) and produces a structure that is partially extended instead of bent. The turn region of representative structures taken from the three families of conformations obtained from the ensemble calculations is shown in Figure 6. The three families are judged to have roughly the same potential energy based on a full force field calculation (i.e., *Discover* force field).

Discussion

The micellar environment was effective in inducing an ordered secondary structure in [Thr^{6}]-BK. The peptide adopts a bent structure at the C-terminus, as indicated from characteristic NOEs. The DG calculations identified it as a β-turn of type I. The NOEs observed are qualitatively similar to those reported by Lee[27] in the study of BK in aqueous solution of SDS micelles, although these authors found looser constraints on the relevant distances $Pro^{7}{}_{H^{\alpha}}/Arg^{9}{}_{HN}$ and $Phe^{8}{}_{HN}/Arg^{9}{}_{HN}$. The temperature coefficients provided evidence of a hydrogen-bonded HN for Arg^{9}. β-Turns of different types were identified at the C-terminus of BK only after the DG structures underwent restrained energy minimization or restrained molecular dynamics; the turns are indicated as type I, II, or VII, with severe deviations from ideal values.[27] The differences between the calculated structures are explained by the authors

as arising from the lack of sufficient NOE restraints and from the characteristics of the calculation programs.[27]

The structures calculated for [Thr6]-BK in this study converge to a definitely better defined β-turn at the C-terminus when compared with those calculated for BK. However, this comparison (i.e., the structures calculated here and in the work of Lee et al. for BK) must be carried out with great care; the calculations have been carried out with different algorithms and protocols, and as pointed out by Lee and co-workers, the detailed structural information of their results is greatly influenced by the DISGEO algorithm and/or in vacuum molecular dynamics simulations. In addition, the experimental conditions differ greatly: Lee et al. used a BK concentration of 16.4 mM and a peptide:micelle ratio of 5, compared with a ratio of 50 used in this study. In theory, this could produce a different association of the peptide with the micelle. Despite these experimental differences, we believe that the largest factor for the more stable conformation observed for [Thr6]-BK is the substitution at position 6 (i.e., Thr6 for Ser6). This is evidenced by the presence of a greater number of NOEs in the region of the β-turn involving Thr6.

The information obtained in this conformational study of [Thr6]-BK is completed by the application of the ensemble calculations. In this manner, not only was the conformational flexibility assessed but the preferred conformations contributing to the NMR observables were also determined. Most of the structures are found to populate a β-turn of type I or II in the residues 6−9. This particular structure has been predicted as favorable for BK from molecular dynamics studies by Perez[60] and with simulated annealing calculations by Salvino.[61] There is evidence of a tendency of BK to fold into a bent structure at the C-terminus also in solvent systems such as dioxane:water, 9:1, and dimethyl sulfoxide and in the presence of lisophosphatidylcholine micelles.[62] The existence of a well-defined β-turn in [Thr6]-BK in the presence of a membrane mimetic, together with the data on the peptide biological activity, substantiates the hypothesis that this structural motif is determinant for high receptor affinity and activity.

In addition to the conformational studies on BK itself, data are available on a number of peptide antagonists. A correlation has been hypothesized between a C-terminal β-turn and the antagonistic effect,[10,28−33] but it is not yet clear if the antagonist maintains this conformation upon binding to the receptor. This conclusion is supported by the results on the highly potent BK antagonist Hoe 140 (Hoechst-140: D-Arg0-Arg1-Pro2-Hyp3-Gly4-Thi5-Ser6-D-Tic7-Oic8-Arg9) which adopts a C-terminal turn in water/SDS micelles solution identified as a β-turn type II′ from restrained molecular dynamics simulations in a biphasic membrane mimetic (H_2O/CCl_4).[25] In the accompanying paper the two β-turn-containing conformations obtained from the ensemble calculations are studied by molecular dynamics in the biphasic membrane mimetic. This will allow for the characterization of the peptide utilizing a full force field in the presence of a two-phase environment, similar to that utilized in solution, and for the determination of the peptide orientation relative to the membrane−interface.

Acknowledgment. The authors wish to thank Prof. R. Rocchi and Dr. M. Gobbo (University of Padova) for the [Thr6]-bradykinin samples and many helpful discussions.

References

(1) Farmer, S. G.; Burch, R. M. L. R. In *Bradykinin Antagonists, Basic and Clinical Research*; Burch, R. M., Ed.; Marcel Dekker: New York, 1991; pp 1−31.
(2) Stewart, J. M. Bradykinin Antagonists: Development and Applications. *Biopolymers* **1995**, *37*, 143−155.
(3) Benetos, A.; Gavras, H.; Stewart, J. M.; Vavrek, R. J.; Hatinoglou, S.; Gavras, I. Vasodepressor Role of Endogenous Bradykinin Assessed by a Bradykinin Antagonist. *Hypertension* **1986**, *8*, 971−974.
(4) Carbonell, L. F.; Carreterro, O. A.; Stewart, J. M.; Scicli, A. G. Effect of a Kinin Antagonist on the Acute Antihypertensive Activity of Enalaprilat in Severe Hypertension. *Hypertension* **1988**, *11*, 239−243.
(5) Regoli, D.; Barabe, J. Pharmacology of Bradykinin and Related Kinins. *Pharmacol. Rev.* **1980**, *32*, 1−46.
(6) Steranka, L. R.; Manning, D. C.; De Haas, C. J.; Ferkany, J. W.; Borosky, S. A.; Connor, J. R.; Vavrek, R. J.; Stewart, J. M.; Snyder, S. H. Bradykinin as a Pain Mediator: Receptors Are Localized to Sensory Neurons, and Antagonists Have Analgesia Action. *Proc. Natl. Acad. Sci. U.S.A.* **1988**, *85*, 3245−3249.
(7) Kyle, D. J.; Burch, R. M. A Survey of Bradykinin Receptors and Their Antagonists. *Curr. Opin. Invest. Drugs* **1993**, *2* (1), 5−20.
(8) Proud, D.; Reynolds, C. J.; Lacapra, S.; Schotka, A.; Lichtenstein, L. M.; Naclerio, R. M. Nasal Provocation with Bradykinin Induces Symptoms of Rhinovirus and a Sore Throat. *Am. Rev. Respir. Dis.* **1988**, *137*, 613−616.
(9) Naclerio, R. M.; Proud, D.; Lichtenstein, L. M.; Sobotka-Kagey, A.; Hemdley, J. O.; Sorrentino, J..; Gwaltney, J. M. Kinins Are Generated During Experimental Rhinovirus Colds. *J. Infect. Dis.* **1988**, *157*, 133−142.
(10) Kyle, D. J.; Martin, J. A.; Farmer, S. G.; Burch, R. M. Design and Conformational Analysis of Several Highly Potent Bradykinin Receptor Antagonists. *J. Med. Chem.* **1991**, *34*, 1230−1233.
(11) Romano, R.; Dufresne, M.; Prost, M. C.; Bali, J. P.; Bayerl, T. M.; Moroder, L. Peptide Hormone-Membrane Interactions. Intervesicular Transfer of Lipophilic Gastrin Derivatives to Artificial Membranes and their Bioactivities. *Biochim. Biophys. Acta* **1993**, *1145*, 235−242.
(12) Moroder, L.; Romano, R.; Guba, W.; Mierke, D. F.; Kessler, H.; Delporte, C.; Winand, J.; Christophe, J. New Evidence for a Membrane-Bound Pathway in Hormone Receptor Binding. *Biochemistry* **1993**, *32*, 13551−13559.
(13) Sargent, D. F.; Schwyzer, R. Membrane Lipid Phase as Catalyst for Peptide-Receptor Interactions. *Proc. Natl. Acad. Sci. U.S.A.* **1986**, *83*, 5774−5778.
(14) Schwyzer, R. Estimated Conformation, Orientation, and Accumulation of Dynorphin A-(1−13)-Tridecapeptide on the Surface of Neutral Lipid Membranes. *Biochemistry* **1986**, *25*, 4281−4286.
(15) Schwyzer, R. How Do Peptides Interact with Lipid Membranes and How Does This Affect Their Biological Activity? *Braz. J. Med. Biol. Res.* **1992**, *25*, 1077−1089.
(16) Wooley, G. A.; Deber, C. M. Peptides in Membranes: Lipid-Induced Secondary Structure of Substance P. *Biopolymers* **1987**, *26*, S109−S121.
(17) Schwyzer, R. In *Natural Products and Biological Activities;* Imura, H.; Goto, T.; Murachi, T.; Nakajima, T.; Eds.; Tokyo Press and Elsevier: Tokyo, 1986; pp 197−207.
(18) Schwyzer, R. Peptide-Membrane Interactions and a New Principle in Quantitative Structure-Activity Relationships. *Biopolymers* **1991**, *31*, 785−792.
(19) Lee, K. H.; Fitton, J. E.; Wüthrich, K. Nuclear Magnetic Resonance Investigation of the Conformation of Delta-Haemolysin Bound to Dodecylphosphocholine Micelles. *Biochim. Biophys. Acta* **1987**, *911*, 144−153.
(20) Bösch, C.; Brown, L. R.; Wüthrich, K. Physicochemical Characterization of Glucagon-Containing Lipid Micelles. *Biochim. Biophys. Acta* **1980**, *603*, 298−312.
(21) Bairaktari, E.; Mierke, D. F.; Mammi, S.; Peggion, E. Conformations of Bombolitins I and III in Aqueous Solutions: Circular Dichroism, 1H NMR, and Computer Simulation Studies. *Biochemistry* **1990**, *29*, 10096−10102.
(22) Brown, L. R.; Bösch, C.; Wüthrich, K. Location and Orientation Relative to the Micelle Surface for Glucagon in Mixed Micelles with Dodecylphosphocholine. *Biochim. Biophys. Acta* **1981**, *642*, 296−312.
(23) Kallick, D. A.; Tessmer, M. R.; Watts, C. R.; Li, C. Y. The Use of Dodecylphosphocholine Micelles in Solution NMR. *J. Magn. Reson. B* **1995**, *109*, 605−665.
(24) McDonnell, P. A.; Opella, S. J. Effect of Detergent Concentration on Multidimensional Solution NMR Spectra of Membrane Proteins in Micelles. *J. Magn. Reson. B* **1993**, *102*, 120−125.

(25) Guba, W.; Haessner, R.; Breiphol, G.; Henke, S.; Knolle, J.; Santagada, V.; Kessler, H. Combined Approach of NMR and Molecular Dynamics within a Biphasic Membrane Mimetic: Conformation and Orientation of the Bradykinin Antagonist Hoe 140. *J. Am. Chem. Soc.* **1994**, *116*, 7532−7540.
(26) Papavoine, C. H. M.; Konings, R. N. H.; Hilbers, C. W.; van den Ven, F. J. M. Location of M13 Coat Protein in Sodium Dodecyl Sulfate Micelles As Determined by NMR. *Biochemistry* **1994**, *33*, 12990−12997.
(27) Lee, S. C.; Russel, A. F.; Laidig, W. D. Three Dimensional Structure of Bradykinin in SDS Micelles. *Int. J. Pept. Protein Res.* **1990**, *35*, 367−377.
(28) Kyle, D. J.; Hicks, R. P.; Blake, P. R.; Klimowski, V. J. In *Bradykinin Antagonists, Basic and Clinical Research*; Burch, R. M.; Ed.; Marcel Dekker: New York, 1991; pp 131−146.
(29) Kyle, D. J.; Martin, J. A.; Burch, R. M.; Carter, J. P.; Lu, S.; Meeker, S.; Prosser, J. C.; Sullivan, J. P.; Togo, J.; Noronha-Blob, L.; Sinsko, J. A.; Walters, R. F.; Whaley, L. W.; Hiner, R. N. Probing the Bradykinin Recepor: Mapping the Geometric Topography Using Ethers of Hydroxyproline in Novel Peptides. *J. Med. Chem.* **1991**, *34*, 2649−2653.
(30) Kyle, D. J.; Green, L. M.; Blake, P. R.; Smithwick, D.; Summers, M. F. A Novel β-turn Mimetic Useful for Mapping the Unknown Topology of Peptide Receptors. *Pept. Res.* **1992**, *5*, 206−209.
(31) Chakravarty, S.; Wilkins, D.; Kyle, D. J. Design of Potent, Cyclic Peptide Bradykinin Receptor Antagonists from Conformationally Constrained Linear Peptides. *J. Med. Chem.* **1993**, *36*, 2569−2571.
(32) Kyle, D. J.; Blake, P. R.; Smithwick, D.; Green, L. M.; Martin, J. A.; Sinsko, J. A.; Summers, M. F. NMR and Computational Evidence that High Affinity Bradykinin Receptor Antagonists Adopt C-terminal β-turns. *J. Med. Chem.* **1993**, *36*, 1450−1460.
(33) Liu, X.; Stewart, J. M.; Gera, L.; Kotovych, G. Proton Magnetic Resonance Studies of Bradykinin Antagonists. *Biopolymers* **1993**, *33*,1237−1247.
(34) Piek, T.; Buitenhuis, A.; Simon Thomas, R. T.; Ufkes, J. G. R. Smooth Muscle Contracting Compounds in the Venom of Megascolia Flavifrons (Hym. Scoliidae) with Notes on the Stinging Behavior. *Comp. Biochem. Physiol.* **1983**, *75C*, 145−152.
(35) Piek, T. Neurotoxic Kinins from Wasp and Ant Venoms. *Toxicon* **1991**, *29*, 139−149.
(36) Hue, B.; Piek, T. In *Neurotox '88, Molecular Basis of Drugs and Pesticide Action*; Lunt, G. G.; Ed.; Elsevier: Amsterdam, 1988; p 27.
(37) Hue, B.; Piek, T. Irreversible Presynaptic Activation-Induced Block of Transmission in the Insect CNS by Hemicholinium-3 and Threonine-6-Bradykinin. *Comp. Biochem. Physiol.* **1989**, *93C*, 87−89.
(38) Gobbo, M.; Biondi, L.; Filira, F.; Piek, T.; Rocchi, R. Cyclic Analogues of Thr^6-Bradykinin, N^{ϵ}-Lys-Bradykinin and *endo*-Lys$^{8\alpha}$-Vespulakinin 1. *Int. J. Pept. Protein Res.* **1995**, *45*, 459−465.
(39) Tanford, C. *The Hydrophobic Effect: Formation of Micelles and Biological Membranes*; John Wiley & Sons: New York, 1980; p 54.
(40) Rance, M.; Sørensen, O. W.; Bodenhausen, G.; Wagner, G.; Ernst, R. R.; Wüthrich, K. Improved Spectral Resolution in COSY Proton NMR Spectra of Proteins Via Double Quantum Filtering. *Biochem. Biophys. Res. Commun.* **1983**, *117*, 458−479.
(41) Braunschweiler, L.; Ernst, R. R. Coherence Transfer by Isotropic Mixing: Application to Proton Correlation Spectroscopy. *J. Magn. Reson.* **1983**, *53*, 521−528.
(42) Bax, A.; Davis, D. G. MLEV-17 Based Two-Dimensional Homonuclear Magnetization Transfer Spectroscopy. *J. Magn. Reson.* **1985**, *65*, 355−360.
(43) Jeener, J.; Meier, B. H.; Bachmann, P.; Ernst, R. R. Investigation of Exchange Processes by Two-Dimensional NMR Spectroscopy. *J. Chem. Phys.* **1979**, *71*, 4546−4553.
(44) Macura, S.; Huang, Y.; Suter, D.; Ernst, R. R. Two-Dimensional Chemical Exchange and Cross-Relaxation Spectroscopy of Coupled Nuclear Spins. *J. Magn. Reson.* **1981**, *43*, 259−281.
(45) States, D. J.; Haberkorn, R. A.; Ruben, D. J. A Two-Dimensional Nuclear Overhauser Experiment with Pure Absorption Phase in Four Quadrants. *J. Magn. Reson.* **1982**, *48*, 286−292.
(46) Bothner-By, A. A.; Stephens, R. L.; Lee, J.; Warren, C. D.; Jeanloz, R. W. Structure Determination of a Tetrasaccharide: Transient Nuclear Overhauser Effect in The Rotating Frame. *J. Am. Chem. Soc.* **1984**, *106*, 811−813.
(47) Kessler, H.; Griesinger, C.; Kerssebaum, R.; Wagner, K.; Ernst, R. R. Separation of Cross-Relaxation and J Cross-Peaks in 2D Rotating-Frame NMR Spectroscopy. *J. Am. Chem. Soc.* **1987**, *109*, 607−609.
(48) Muller, L. P. E. COSY, a Simple Alternative to E. COSY. *J. Magn. Reson.* **1987**, *72*, 191−196.
(49) Wüthrich, K.; Billeter, M.; Braun, W. Pseudo-Structures for the 20 Common Amino Acids for Use in Studies of Protein Conformations by Measurements of Intramolecular Proton-Proton Distance Constraints with Nuclear Magnetic Resonance. *J. Mol. Biol.* **1983**, *169*, 949−961.
(50) Havel, T. F. An Evaluation of Computational Strategies for Use in the Determination of Protein Structure from Distance Constraints Obtained by Nuclear Magnetic Resonance. *Prog. Biophys. Mol. Biol.* **1991**, *56*, 43−78.
(51) Crippen, G. M.; Havel, T. F. *Distance Geometry and Molecular Conformation*; Research Studies Press Ltd.: Somerset, England, 1988.
(52) Kaptein, R.; Boelens, R.; Scheek, R. M.; van Gunsteren, W. F. Protein Structures from NMR. *Biochemistry* **1988**, *27*, 5389−5395.
(53) Scheek, R. M.; van Gunsteren, W. F.; Kaptein, R. In *Methods in Enzymology*; Oppenheimer, N. J.; James, T. L. Eds.; Academic Press: New York, 1989; Vol. 177, pp 204−218.
(54) Mierke, D. F.; Geyer, A.; Kessler, H. Improved Distance Geometry Methods for Conformation of Peptides. *Int. J. Pept. Protein Res.* **1994**, *44*, 325−331.
(55) Mierke, D. F.; Scheek, R. M.; Kessler, H. Coupling Constant Restraints in Ensemble Calculations. *Biopolymers* **1994**, *34*, 559−563.
(56) Wüthrich, K.; Billeter, M.; Braun, J. Polypeptides Secondary Structure Determination by Nuclear Magnetic Resonance Observation of Short Proton-Proton Destances. *J. Mol. Biol.* **1984**, *180*, 715−740.
(57) Reed, J.; Hull, W. E.; Lieth, C. W.; Kubler, D.; Subai, S.; Kinzel, V. Secondary Structure of the Arg-Gly-Asp Recognition Site in Proteins Involved in Cell-Surface Adhesion. Evidence for the Occurrence of Nested Beta-Bends in The Model Hexapeptide. *Eur. J. Biochem.* **1988**, *178*, 141−154.
(58) Blanco, F. J.; Jiménez, M. A.; Rico, M.; Santoro, J.; Herranz, J.; Nieto, J. L. Tendamistat (12−26) Fragment. NMR Characterization of Isolated Beta-Turn Folding Intermediates. *Eur. J. Biochem.* **1991**, *200*, 345−351.
(59) Dyson, H. J.; Rance, M.; Houghteen, R. A.; Lerner, R. A.; Wright, P. E. Folding of Immunogenic Peptide Fragments of Proteins in Water Solution. I. Sequence Requirements for the Formation of a Reverse Turn. *J. Mol. Biol.* **1988**, *201*, 161−200.
(60) Perez, J. J.; Sanchez, Y. M.; Centeno, N. B. *J. Pept. Sci.* **1995**, *1*, 227−235.
(61) Salvino, J. M.; Seoane, P. R.; Dolle, R. E. Conformational Analysis of Bradykinin by Annealed Molecular Dynamics and Comparison to NMR Derived Conformations. *J. Comput. Chem.* **1993**, *14*, 438−444.
(62) Young, J. K.; Hicks, R. P. NMR and Molecular Modeling investigations of the Neuropeptide Bradykinin in Three Different Solvent Systems: DMSO, 9:1 Dioxane/Water, and in the Presence of 7.4 mM Lyso Phosphatidylcholine Micelles. *Biopolymers* **1994**, *34*, 611−623.

JM9605391